Mpl traffics to the cell surface through conventional and unconventional routes

Cédric Cleyrat[1, 2], Anza Darehshouri[1], Mara P. Steinkamp[1], Mathias Vilaine[2], Daniela Boassa[3], Mark H. Ellisman[3], Sylvie Hermouet[2] and Bridget S. Wilson[1]

Supplemental Figure

Supplemental Figure 1: Correlated fluorescent and electron microscopy of mKO2-miniSOG tagged Mpl proteins. A) Schematic representation of the DNA construct coding for the $Mpl^{mKO2\text{-}miniSOG}$ fusion protein. B-C) Examples of K562 and HEL cells transiently expressing $Mpl^{mKO2\text{-}miniSOG}$ and imaged using both mKO2 and miniSOG fluorescent properties. D-E) Correlated light, before and after photo-oxidation, and electron micrograph images from a single K562 (B) or HEL (C) cell. Scale bars = 5 μm.

Supplemental Figure 2: TEM images of control experiments on K562 and HEL cells showing the absence of dark precipitate in the absence of photo-oxidation or in the absence of $Mpl^{mKO2\text{-}miniSOG}$. A-B) TEM images of un-transfected K562 (A) or HEL (B) cells. No dark precipitate can be observed. C-D) TEM images of K562 (C) or HEL (D) cells transfected with $Mpl^{mKO2\text{-}miniSOG}$ in absence of photo-oxidation showing the absence of obvious dark precipitate. E-F) High magnification TEM images of un-transfected K562 (E) or HEL (F) cells submitted to the photo-oxidation process. Small dark spots can be observed in vesicles identified as lysosomes and are probably due to the presence of oxidative enzymes. The same observation has been made concerning mitochondria's membranes. Scale bars = 1 μm (A-D) or 100 nm (E-F).

Supplemental Figure 3: TEM micrographs showing Mpl-positive structures budding from ER in HEL A-C), and K562 (D-F) cells. A,D) Involuted ER compartments in non-photo-oxidized HEL (A) and K562 (D) cells. B,E) double membrane autophagosomes (arrows) in HEL (B) and K562 (E) cells containing dark precipitates produced as a result of $Mpl^{mKO2\text{-}miniSOG}$ photo-oxidation. Multi lamellar body (black arrowhead) in HEL (C) and multivesicular bodies (white arrowheads) in K562 cells (F). Scale bar = 100 nm.

Supplemental Figure 4: Intracellular Mpl^{eCFP} co-localizes with autophagosomes and autolysosomes. A-B) K562 (A) and HEL (B) cells stably expression $LC3^{mRFP\text{-}GFP}$ were co-transfected with Mpl^{eCFP}. Cells were then stimulated, or not, with Tpo at 25ng/mL for the indicated time. In both cell lines, traces of fluorescence profile (white arrows) are showing the presence of Mpl^{eCFP} in autophagosomes (black arrow heads) and in autolysosomes (violet arrow heads). Scale bars = 5 μm.

Supplemental Figure 5: Alexa Fluor-488 labeling of human recombinant Tpo. A) Non-reducing PAGE experiment showing efficiently labelled Tpo with alexa fluor-488 dye. The labeling reaction was done as described in the Materiel & Methods section. We can also note the presence of trace contamination. B) Confocal image of K562 cells transiently expressing $Mpl^{mOrange2}$ and stimulated with Tpo chemically labeled with Alexa Fluor-488 dye (AF488). Tpo-488 binds specifically to $Mpl^{mOrange2}$ and upon activation the receptor is internalized. As plotted on the attached fluorescence graph, there is a very good co-localization of $Mpl^{mOrange2}$ and Tpo-488 at the plasma membrane as well as in endocytic vesicles (black arrow heads). Intracellular vesicles containing $Mpl^{mOrange2}$ only (red arrow heads) were also easily identified. As a control, white stars indicate non-transfected cells that do not bind Tpo-AF488, showing the specificity of the binding. Scale bars = 5 μm.

Supplemental Figure 6: A) Western blot analysis and quantification of HEL and $K562^{Mpl\text{-}mKO2}$ total lysate (prior to surface IP as presented in Figure 7A) probed with an anti-Mpl and an anti-actin antibodies. The quantification of this western blot is shown below and show that at the total lysate level there is no change in the distribution of Mpl forms. B) The same total lysates as in A) were run on the same gel as the surface IP lysate shown in Figure 7A and the membranes were probed with an anti-Grb2 and an anti-actin antibodies. This western blot shows the minor contamination of the surface IP proteins by total lysate proteins. C) Semi-quantitative RT-PCR assay showing the absence of endogenous *MPL* transcript in K562 cells, transfected or not with $Mpl^{mKO2/mOrange2}$. *RPLP0* is used as a housekeeping gene. ***Methods for (C):*** $5x10^6$ cells of each cell line tested (HEL, K562, $K562^{Mpl\text{-}mOrange2}$ and $K562^{Mpl\text{-}mKO2}$) were lysed, and total RNA were extracted using a Nucleospin RNA extraction kit (Macherey-Nagel, Düren, Germany). Qualities of total RNA extracts were

then assessed by spectrophotometry and agarose gel electrophoresis. Normalized quantities of RNA were then submitted to an oligodT RT-PCR using a first strand cDNA synthesis kit (Life Technologies, Carlsbad, CA, USA) following the manufacturer recommendations. 5 μL of a 1/10 dilution (1/10 for *RPLP0*) of the newly synthesized cDNA were used to perform a PCR amplification specific for endogenous *MPL*, recombinant *MPL* and *RPLP0* (housekeeping gene) using the primers listed below. The PCR reactions were done using a platinum Taq DNA polymerase (Life Technologies, Carlsbad, CA, USA) as follows: Activation at 95°C for 5 minutes; 35 cycles of 1) Denaturation at 95°C for 5 minutes, 2) Hybridization at 62°C for 30 seconds, 3) Elongation at 72°C for 45 seconds; elongation at 72°C for 5 minutes. For PCR reactions that were submitted to only 20, 25 or 30 cycles, the PCR tubes were removed from the thermocycler during the elongation step of the corresponding cycle number and then incubated 5 minutes in a water bath at 72°C to ensure the full extension of the DNA strands. Finally, PCR reactions were cooled down to 4°C, mixed with 10x loading buffer and 15 μL of each PCR were loaded on a 1.5% agarose gel. After migration DNA was stained using the GelRed dye (Biotium, Hayward, CA, USA) and imaged with a Bio-Rad ChemiDoc XRS+ (Bio-Rad, Hercules, CA, USA). ***Primers:*** **1)** Amplification of the endogenous *MPL* gene : $Fwd_{common\ hMPL}$ 5'-CACTTCCAGACCTGCACCGG-3', $Rvse_{3'UTR\text{-}hMPL}$ 5'-GGGGAACTAATTGAAGTAGTCTCAAGAGTAAATGGG -3', Amplicon size = 658 bp. **2)** Amplification of recombinant *MPL-mOrange2* :$Fwd_{common\ hMPL}$ 5'-CACTTCCAGACCTGCACCGG-3', $Rvse_{MPL\text{-}mOrange2}$ 5'-GGAGTCCTGGGTCACGGTC-3', Amplicon size = 662 bp. **3)** Amplification of recombinant *MPL-mKO2* :$Fwd_{commonhMPL}$ 5'-CACTTCCAGACCTGCACCGG-3', $Rvse_{MPL\text{-}mKO2}$ 5'-CCACATCAGCCTGAGGGGC-3', Amplicon size = 656 bp. **4)** Amplification of RPLP0 :Fwd_{hRPLP0} 5'-CTCTGGAGAAACTGCTGCCTCATATCC-3', $Rvse_{hRPLP0}$ 5'-AGCAGCAGC AGGAGCAGCTGTG-3', Amplicon size = 656 bp.

Cleyrat et al. Supplemental Figure 1

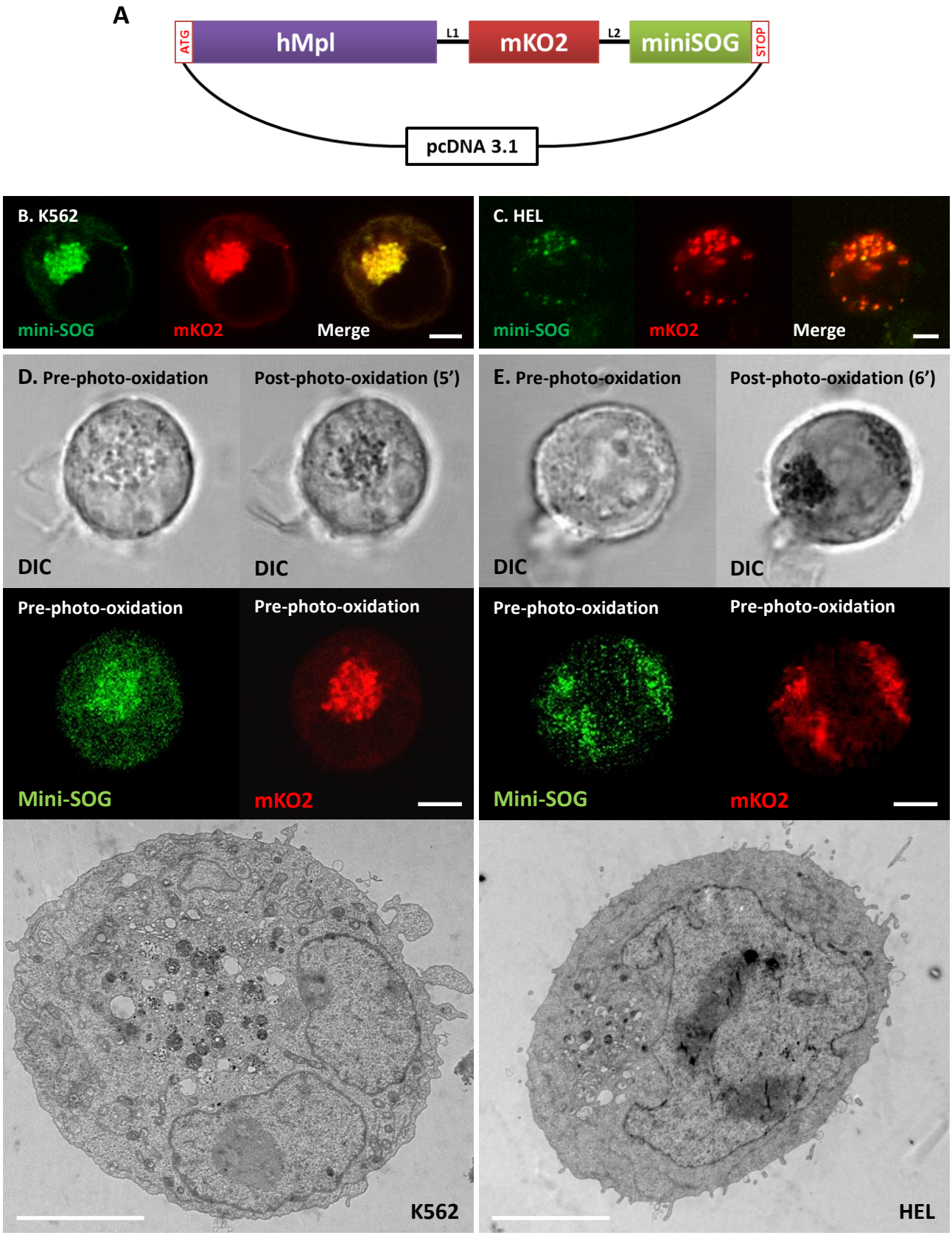

bars = 5 μm

Cleyrat et al. Supplemental Figure 2

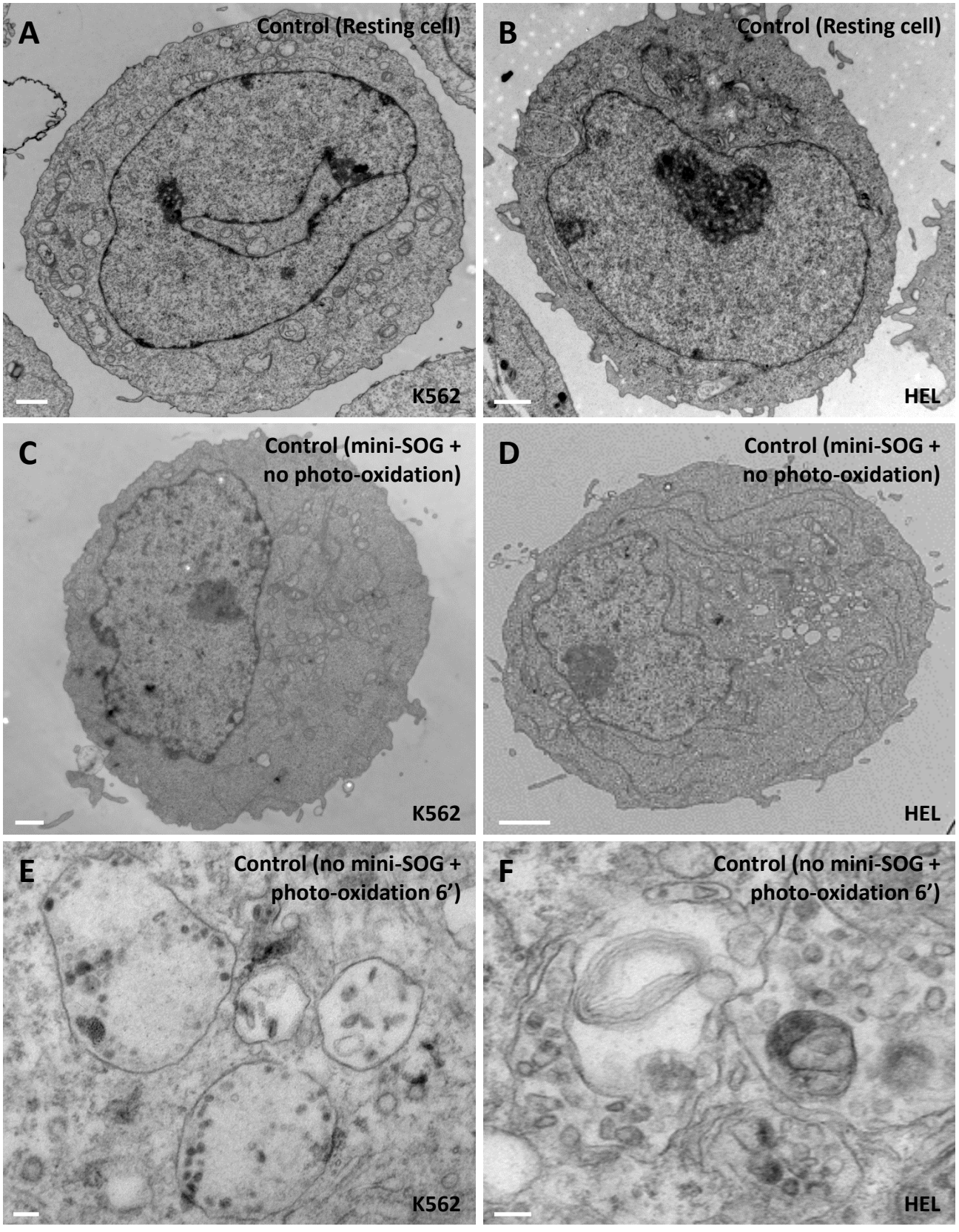

bars = 1 μm (low mag
or 100 nm (high mag)

Cleyrat et al. Supplemental Figure 3

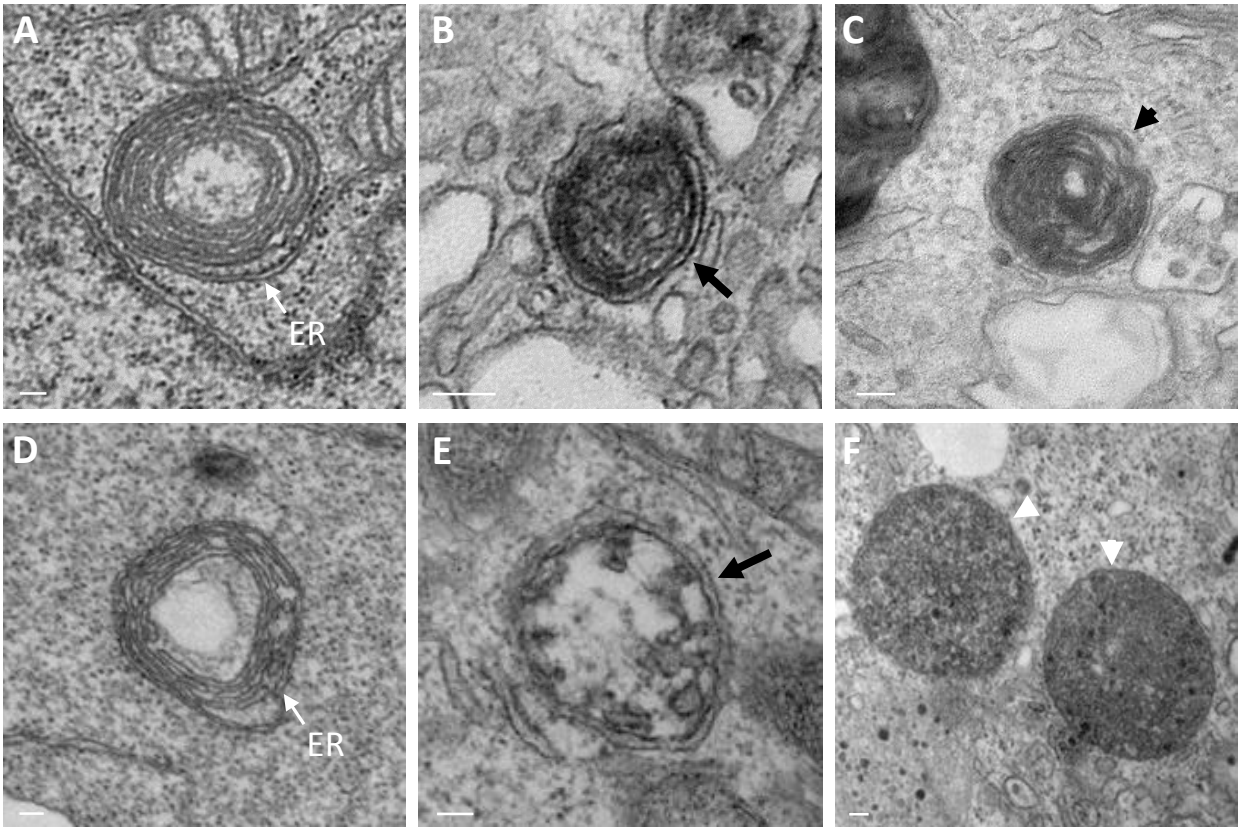

bars = 100 nm

Cleyrat et al. Supplemental Figure 4

A. K562 cells

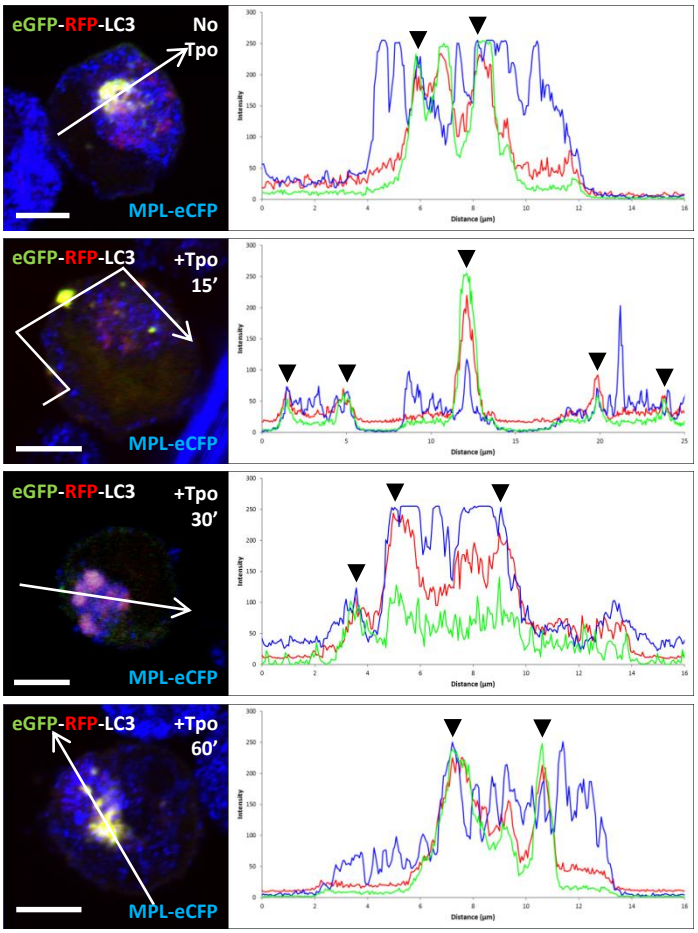

B. HEL cells

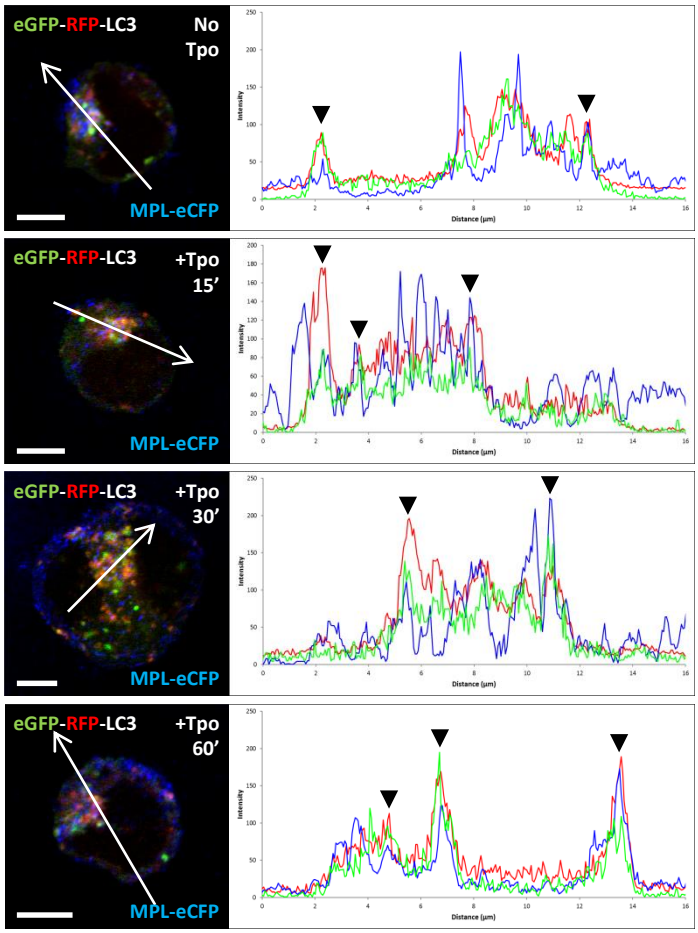

bars = 5 µm

Cleyrat et al. Supplemental Figure 5

A. Tpo labeling with AF488

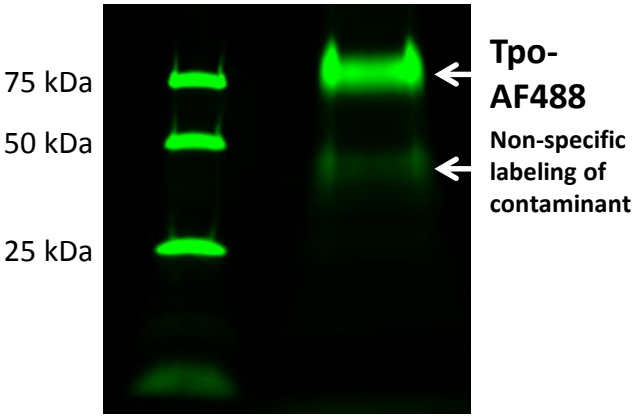

B. Stimulation with Tpo-AF488

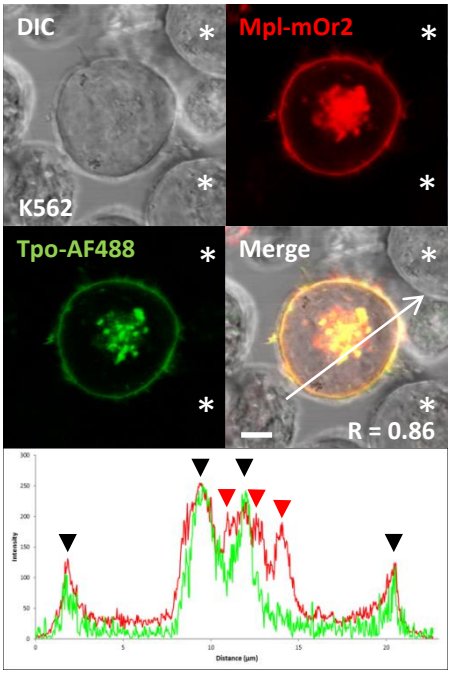

bar = 5 µm

Cleyrat et al. Supplemental Figure 6